

# **Out-of-plane fragility of URM parts and components based on time-history analysis—comparison to simplified force-based approaches**

**J. Vaculik<sup>1,3</sup> and M.C. Griffith<sup>2,3</sup>**

1. Corresponding Author. Research Associate, School of Civil, Environmental and Mining Engineering, University of Adelaide. Email: jaroslav.vaculik@adelaide.edu.au
2. Professor, School of Civil, Environmental and Mining Engineering, University of Adelaide. Email: michael.griffith@adelaide.edu.au
3. Bushfire and Natural Hazards Cooperation Research Centre, Australia.

## **Abstract**

This paper presents a technique for constructing analytical fragility curves for generic URM components such as parapets and façade walls subjected to out-of-plane actions. The technique implements a nonlinear time-history-analysis (THA) that computes the wall's displacement history under generic shaking input. The model defines the wall's capacity by a force-displacement model that neglects tensile bond strength and assumes that all resistance comes from rocking stability and, where applicable, friction. Synthetic accelerograms compatible with the AS 1170.4-2007 soil class D spectrum were used as the ground motion, and the acceleration input applied at the component level was computed by a precursor THA of the building to account for its motion-filtering influence and height amplification. Fragility curves were generated for several different wall configurations including parapets, one-way and two-way spanning walls. The generated curves are used to examine three alternate force-based approaches permitted by AS 1170.4. It is shown that the code techniques are unreliable in estimating the ground motion intensity to cause collapse, and that they are in some instances overly conservative (uneconomical) while being unconservative in others.

**Keywords:** unreinforced masonry; out-of-plane; time-history-analysis; fragility curves; force-based assessment

## INTRODUCTION

Out-of-plane (OOP) failure of component walls such as parapets and building facades is the most common and life-threatening form of failure in unreinforced masonry (URM) buildings in earthquake. A major challenge faced by design practitioners in performing OOP wall assessment in existing URM buildings is that conventional force-based (FB) assessment relies on accurately knowing the tensile bond strength of the masonry. Reliably quantifying bond strength in existing buildings however is costly and intrusive, and furthermore, recent field studies have demonstrated that in aged buildings it can often be negligible (Derakhshan et al, 2018; Burton et al, 2019) to the point where it offers negligible benefit to seismic resistance.

There is therefore strong impetus to develop alternate assessment techniques not reliant on bond strength as an input, that in turn define the wall's force-displacement ( $F$ - $\Delta$ ) capacity in terms of gravity stabilisation effects. Such assessment approaches are still implementable in either a force-based (FB) (e.g. D'Ayala and Speranza, 2003) or displacement-based (DB) format (Doherty et al, 2002; Lagomarsino, 2015; NZSEE, 2017); however, since OOP wall failure is governed by displacement instability rather than exceedance of force capacity, it is commonly recognised that the latter is a conceptually more justifiable framework for collapse prevention.

Force-based design still continues to be the most commonly used technique for seismic *assessment* (i.e. in existing buildings) and *design* (in new buildings) of OOP walls, and remains the only technique catered for in the Australian earthquake code AS 1170.4 (Standards Australia, 2018). The principle of FB design is to ensure that the wall's force capacity exceeds the force demand due to the earthquake—this approach is overly conservative (uneconomical) since it effectively limits wall deformation to the relatively small displacement at which the peak force is achieved ( $\Delta_{ry}$  in Figure 1), and neglects the wall's reserve displacement capacity up to the actual point of instability ( $\Delta_{ru}$ ). By contrast, DB design takes advantage of the wall's full displacement capacity, thus leading to a more realistic estimate of motion intensity to cause collapse.

While there is a growing shift away from FB toward DB design for OOP URM components in certain parts of the world such as Italy and NZ (NZSEE, 2017), a limitation of the current state-of-the-art is that it is yet to be fully generalised to generic wall boundary conditions—particularly walls in two-way bending. This still requires considerable research effort: experimental verification of a time-history analysis (THA) for predicting the component's dynamic response under generic excitation; characterisation of realistic component excitation motions by accounting for URM buildings' filtering effects; and translation of these findings into a reliable but simple-to-use desktop method using equivalent-linearisation principles.

Considerable progress toward this goal has already been made by research teams worldwide, including the authors through the development of a  $F$ - $\Delta$  model applicable to one- or two-way spanning walls (Vaculik and Griffith, 2017) that can act as input into a THA. The objective of this paper is to use this model to develop fragility curves for typical wall configurations, and by doing so, to gain insight into the expected behaviour and improvement in design economy that could be achieved through a DB procedure.

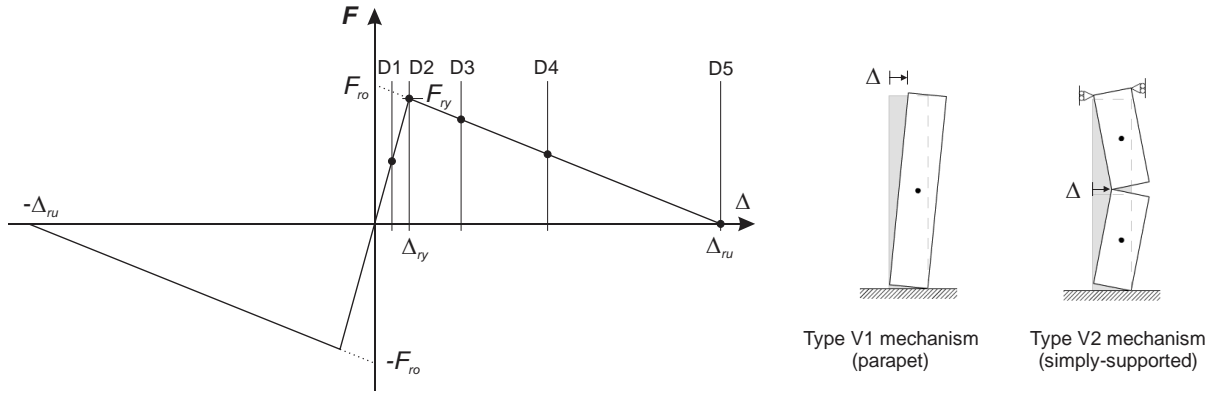


Figure 1:  $F$ - $\Delta$  model for generic wall components under OOP actions, indicating damage levels D1–D5. Shows the elastic rocking component only (inelastic frictional component not shown).

## NONLINEAR TIME-HISTORY ANALYSIS

It is generally recognised that nonlinear THA provides the most accurate prediction of dynamic structural response provided that the model incorporates an accurate representation of the system's dynamic properties, in particular its  $F$ - $\Delta$  behaviour. Therefore, nonlinear THA will be used to construct fragility curves for OOP wall components and to serve as a benchmark for assessing the reliability of alternate force-based code approaches.

The dynamic OOP response of component walls with respect to generic shaking input is computed using a nonlinear time-history analysis using the framework described in Vaculik and Griffith (2008). The method applies the substitute structure approach where the wall is treated as a single-degree-of-freedom (SDOF) system with nonlinear  $F$ - $\Delta$  behaviour.

The motion of the wall is governed by the equation:

$$F_s(u) + c\dot{u} + m\ddot{u} = -m\ddot{u}_s \quad (1)$$

where  $u$ ,  $\dot{u}$ , and  $\ddot{u}$  are the wall's effective displacement, velocity and acceleration respectively;  $\ddot{u}_s$  is the excitation acceleration at the supports;  $F_s(u)$  is the nonlinear force-displacement model;  $c$  is the damping coefficient; and  $m$  is the wall's mass. The THA is undertaken by solving the equation of motion (1) in its incremental form using the conventional step-by-step algorithm.

### Force-displacement model

The equivalent SDOF approach has been previously applied by Doherty et al (2002) to one-way vertically spanning walls. In the present work, the approach is generalised to walls with any boundary conditions—one- or two-way spanning—by implementing the force-displacement model developed in Vaculik and Griffith (2017). The wall's  $F$ - $\Delta$  model is defined by superimposing: 1) an elastic rocking component incorporating destabilising effects, as shown in Figure 1; and 2) an inelastic friction component modelled as elastoplastic. The latter becomes activated only in walls in two-way bending.

Inputs of the model include the force and displacement capacities  $F_{ro}$  and  $\Delta_{ru}$  in the elastic component (Figure 1), and force capacity  $F_{ho}$  in the elastoplastic frictional component. Each of

these are calculated as a function of the wall’s geometry and boundary conditions using the mechanics-based formulas developed in Vaculik and Griffith (2017). The model ignores any bond strength that the wall may have prior to cracking, thus effectively treating the wall as pre-cracked from the outset. The yield displacement  $\Delta_{ry}$  in the rocking component at which the peak force ( $F_{ry}$ ) is achieved (Figure 1) was taken equal to 10% of the wall’s thickness.

The wall’s actual displacement ( $\Delta$ ) is transformed to an effective SDOF system displacement ( $u$ ), the latter defining the displacement in the equation of motion Eq. (1). This transformation assumes that the wall’s mode shape follows the hinge-line pattern consistent with the crack pattern (refer to Vaculik and Griffith, 2008).

### Damage states

To act as an indicator of the wall’s dynamic performance, five damage states were defined in terms of wall displacement limits as summarised in Table 1.

Table 1: Definition of damage states.

Damage state	Description	Displacement limit	Displacement $\Delta$ in a 110mm thick wall
D1	Slight/minor cracking	50% of $\Delta_{ry}$	6 mm
D2	Peak load capacity, moderate cracking	100% of $\Delta_{ry}$	11 mm
D3	Fully formed collapse mechanism, widening of cracks	25% of $\Delta_{ru}$	28 mm
D4	Near collapse, major spalling and/or sliding along cracks	50% of $\Delta_{ru}$	55 mm
D5	Collapse	100% of $\Delta_{ru}$	110 mm

### Damping

Viscous damping within the THA was handled by keeping the damping ratio  $\xi$  constant and continually updating the damping coefficient [ $c$  in Eq. (1)] using the wall’s instantaneous secant stiffness. The following values of  $\xi$  were used, on the basis of Doherty et al (2002): 3% damping for cantilevering mechanisms, including parapets (V1 in Figure 1); 5% damping for mechanisms in which the top and bottom edges are supported (V2 in Figure 1).

## FRAGILITY CURVES

### Excitation motions

**Ground motion:** A suite of 100, 15-second-long synthetic accelerograms compatible with the AS 1170.4 soil D<sub>e</sub> spectrum were used as the ground motion. The motions are compared to the target code spectrum in Figure 2 in terms of their acceleration and displacement spectra, showing a good match for periods between 0.1sec and 2.5sec. While the peak ground acceleration (PGA) of the accelerograms exceeds the nominal PGA of the target spectrum, the implications of this are inconsequential since both the building and component walls have

periods  $> 0.1$  sec. Similarly, the buildings considered have periods  $< 1$  sec, so the mismatch at long periods is not expected to have a significant influence on the accuracy of the results.

Throughout this paper, the intensity measure (IM) selected for the construction of fragility curves is the regional seismic hazard  $k_p Z$ , where  $k_p$  is the return period factor and  $Z$  is the location factor as defined in AS1170.4. This IM can be interchanged with the nominal PGA according to the formula

$$PGA (g) = k_p Z C_h(T = 0) \quad (2)$$

where, for class D<sub>e</sub> soil:  $C_h(T=0) = 1.1$ .

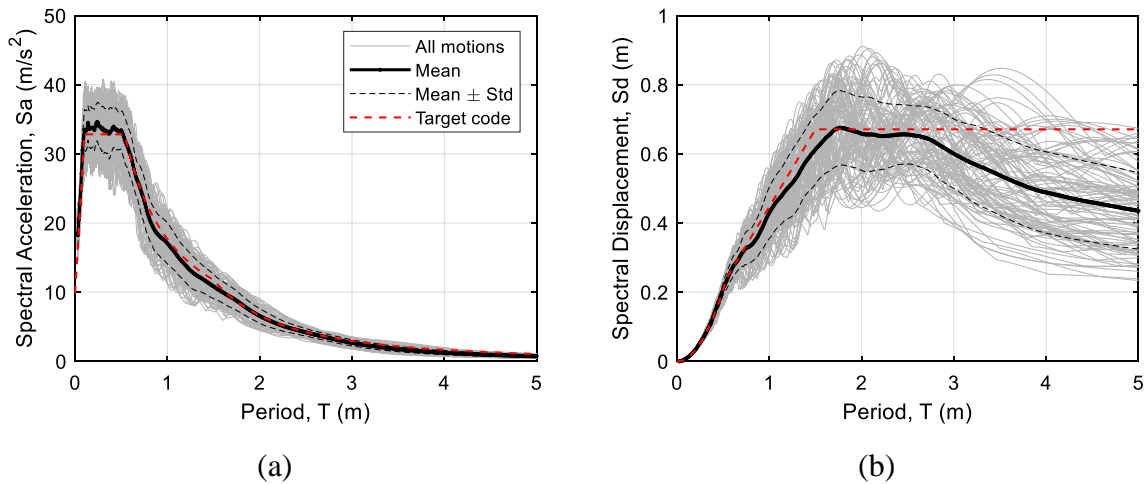


Figure 2: Comparison of the synthetic ground motions with AS1170.4 subsoil D<sub>e</sub> spectra in terms of: (a) spectral acceleration, and (b) spectral displacement.

**Building effects:** The excitation input at the component level is filtered by the dynamics of the building. This was incorporated into the analysis by running a precursor linear THA on an idealised 1-, 2- or 3-storey building, generating floor motions [ $\ddot{u}_s$  in Eq. (1)] that were subsequently used as the excitation for the component walls. The building was treated as a  $n$ -DOF system ( $n$  = number of storeys), with equal mass at each floor, equal horizontal stiffness at each storey, and 5% damping. The first-mode period of the idealised building was set to the value determined using the AS 1170.4 formula

$$T_1 = 1.25 k_t h_n^{0.75} \quad (3)$$

where  $k_t = 0.05$ ; and  $h_n$  is the height of the building, determined by assuming each storey to be 4 m tall. Thus,  $T_1$  was taken as 0.18 sec for a 1-storey building, 0.30 sec for 2-storey, and 0.40 sec for 3-storey.

### Incremental dynamic analysis

An incremental dynamic analysis was performed by running the nonlinear THA under varying ground motion intensity (by linear scaling of the accelerograms). Typical IDA curves—i.e. plots of the maximum wall displacement determined by the THA versus the motion IM—are shown in Figure 3a. The figure considers a reference example of a 1000 mm tall, 230 mm thick

parapet at the roof level of a 1-storey building. From each IDA curve, the motion intensity to achieve a particular damage state can be determined.

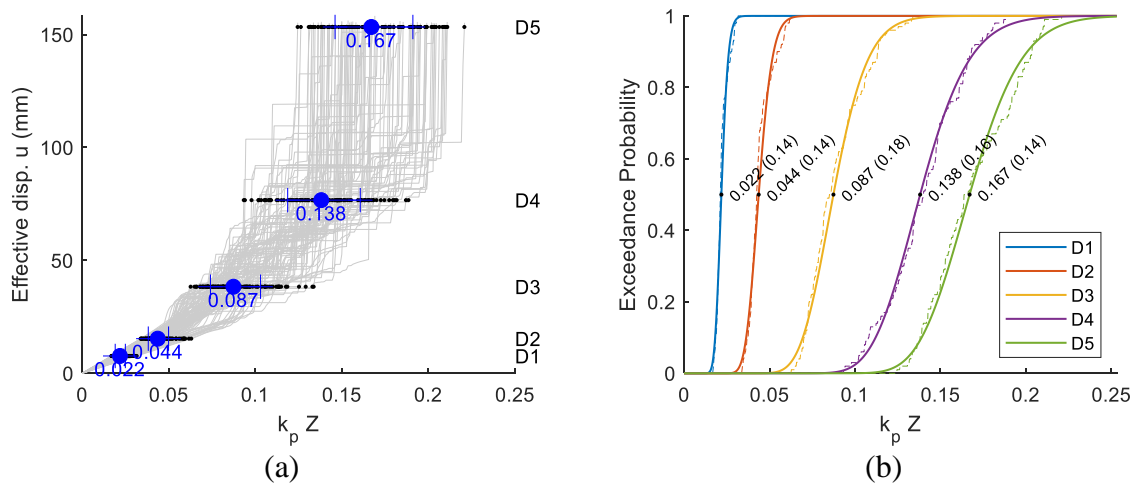


Figure 3: Typical THA results, generated for a 230×1000 mm parapet in a 1-storey building: (a) superimposed IDA curves for 100 different ground motions annotating median IM values; (b) fragility curves,  $\beta$  values given in brackets.

### Fragility curves

Despite being generated for the same target spectrum, each of the 100 synthetic ground motions produces a slightly different IDA curve, requiring the results to be evaluated probabilistically. The lognormal distribution was selected for this purpose, formulating the probability of exceeding a given damage state by the cumulative distribution function (CDF):

$$F(x) = \Phi\left(\frac{\ln x - \mu}{\beta}\right) \quad (4)$$

where  $x$  is the IM of the ground motion;  $\Phi(\dots)$  is the standard normal CDF operator;  $\mu$  is the natural log of the median IM; and  $\beta$  is the standard deviation in the log space. Typical fragility curves, generated for the reference example, are shown in Figure 3b.

### AS 1170.4 FORCED-BASED METHODS

Section 8 of AS 1170.4-2007 gives provision to analyse OOP walls using a force-based design check by treating them as non-structural parts and components. The acceleration demand on the wall,  $a^*$  (in units of g's), is calculated as

$$a^* = a_{\text{floor}} \frac{I_c a_c}{R_c} \quad (5)$$

where  $a_{\text{floor}}$  is the floor acceleration; and  $I_c$ ,  $a_c$ , and  $R_c$  are component importance, amplification and ductility factors, respectively, which the code implies can all be taken as 1. Note that taking  $a_c = 1$  is arguably unconservative since the wall will naturally amplify the motion due to its deformability, which is examined in an upcoming section.

The code effectively permits three alternate ways of computing the floor acceleration term,  $a_{\text{floor}}$ :

**Method 1:** Referred to in AS1170.4 as the *Simple Method*. Floor acceleration is calculated as the PGA times a height amplification factor,  $a_x$ . Factor  $a_x$  varies from 1 at ground level, up to 3 at the top of the building. This approach ignores the building's actual period in the context of dynamic amplification, instead 'lumping' these effects into the single factor  $a_x$ .

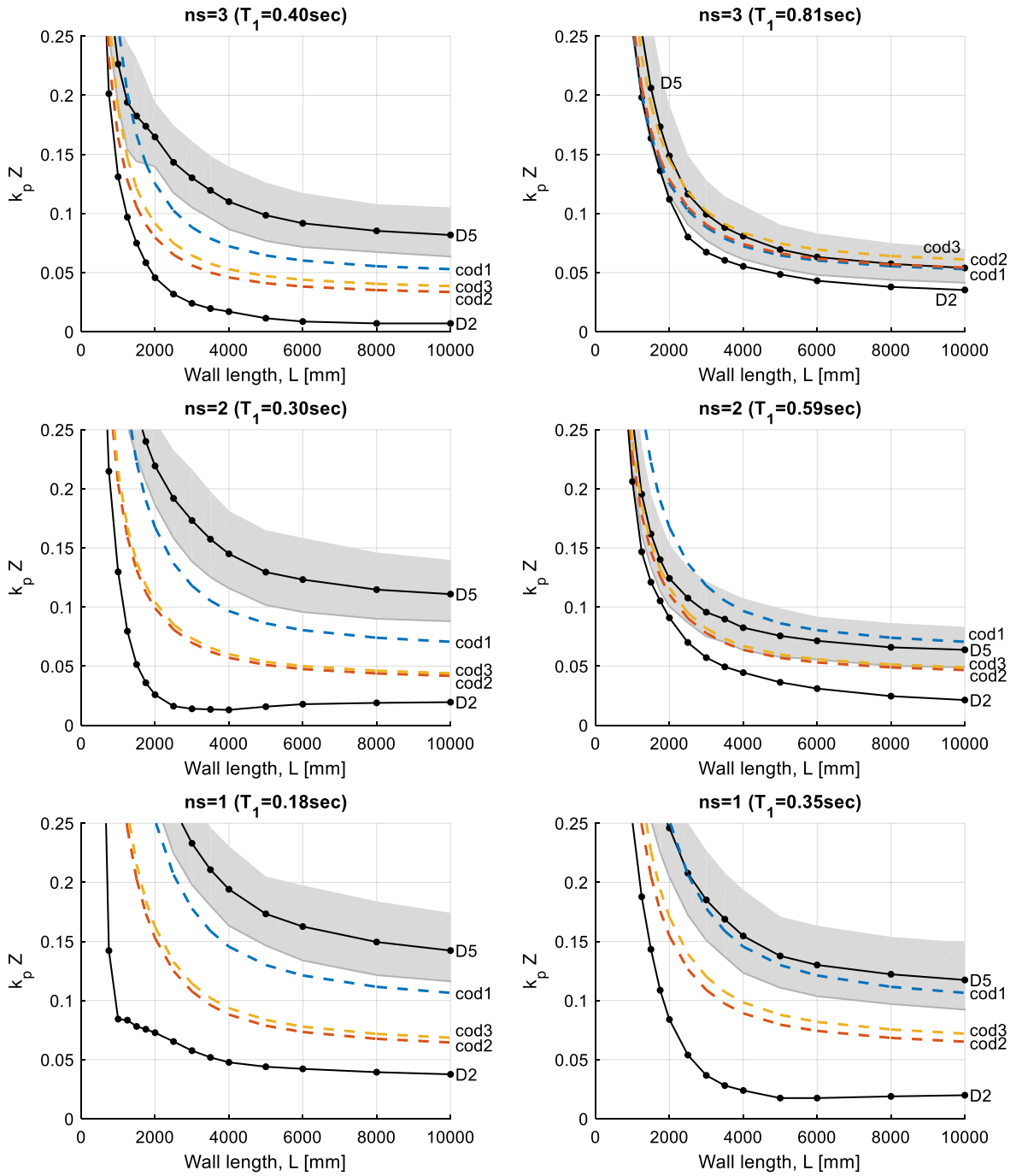
**Method 2:** Floor acceleration is determined from the equivalent static analysis of the building as the floor inertia forced divided by the floor mass. This method takes into account the spectral acceleration of the building at its first mode period ( $T_1$ ) and assumes a predefined mode shape. While the code is not explicit about permitting the floor acceleration to be reduced by  $S_p/\mu$  due to the building's inelastic response, doing so would in the authors' opinion be unsafe, since there is no guarantee that the building becomes inelastic before the wall fails. Hence in this paper  $S_p/\mu$  is taken as 1.

**Method 3:** In this approach the peak floor acceleration is obtained directly from the excitation motion used for the wall THA. This can be treated as the 'exact' representation of the peak floor acceleration in the context of assessing the technique.

To perform the FB design check using each method, the wall's force capacity was taken as the sum of the peak strength of the elastic rocking component,  $F_{ry}$  (see Figure 1), plus the load resistance from the frictional component,  $F_{ho}$ , both of which are calculated using the method described in Vaculik and Griffith (2017).

## RESULTS AND DISCUSSION

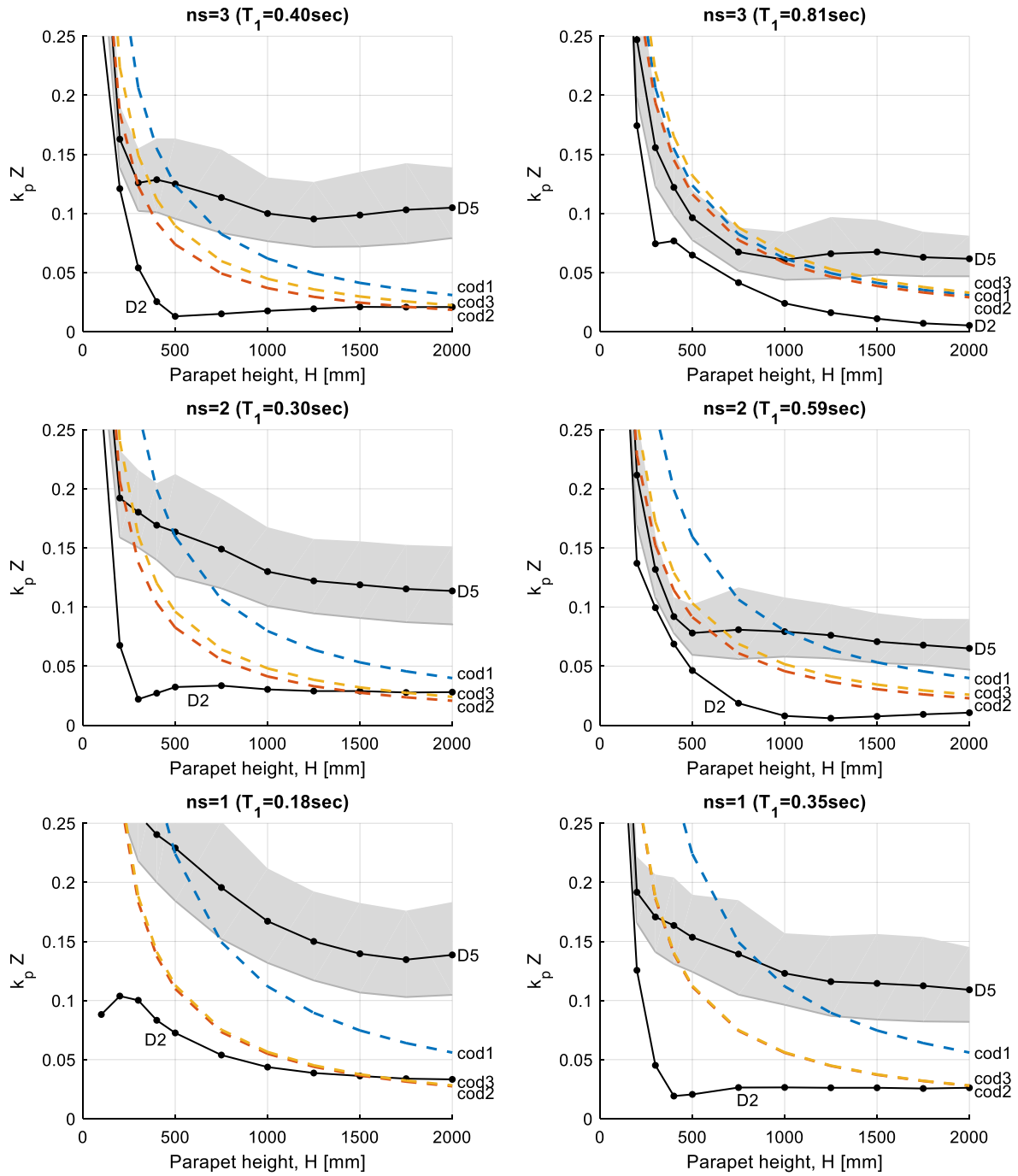
The THA-based fragility analysis was undertaken as part of a parametric study to examine the behaviour of two common types of wall components: a two-way spanning wall with varying horizontal length (Figure 4), and a parapet with varying height (Figure 5); each located in either a 1, 2 or 3-storey building. The vertical axis of these graphs indicates the wall's 'capacity' in terms of the ground motion IM that it can withstand. Two damage levels are considered: the peak force capacity (D2) and collapse (D5). To account for the variability introduced by the randomness of the ground motions, the 5%–95% fractile band for state D5 is shown using grey shading. In the context of engineering design or assessment, the lower (5%) bound for state D5 can be considered a reasonable target for collapse prevention. The three code techniques are shown using dashed lines.



(a) Reference building period [Eq. (3)]

(b) Building period elongated by factor of 2

Figure 4: Capacity of a 110 mm thick, two-way spanning wall pin-supported at all four edges, with height of 3000 mm and variable length,  $L$ . Wall is located on the top storey of a 3-, 2- or 1-storey building ( $ns$  = number of storeys). Black lines denote the fragility medians for damage states D2 (peak strength) and D5 (collapse) as determined from the IDA. Grey-shaded area indicates the corresponding 5%–95% fractile band for D5. The three code methods (1–3 as defined in the text) are indicated by dashed lines: blue = method 1, red=2, yellow=3.



(a) Reference building period [Eq. (3)]

(b) Building period elongated by factor of 2

Figure 5: Capacity of a 230 mm thick parapet with variable height,  $H$ . Refer to caption of Figure 4 for description of the data series.

## Comparison of the code methods

The main difference between the three code methods is the way that they estimate the peak floor acceleration. In this regard, method 3 can be considered to be an ‘exact’ benchmark for the other two methods, since it directly uses the peak floor acceleration determined from the building THA. From Figures 4 and 5 it is seen that method 2 (equivalent static analysis of the building) produces comparable although generally slightly conservative estimates of floor acceleration. By contrast, method 1 (simple method using height amplification factor) is consistently unconservative by a considerable margin. In other words, it under-predicts floor accelerations determined from the linear THA analysis of a  $n$ -DOF building making it potentially unsafe for design. This is concerning to not only the assessment of OOP walls, but also to general seismic design of non-structural parts and components, as this method is routinely used by practicing engineers.

## Design for collapse prevention

Consider the reference analyses shown in parts (a) of Figures 4 and 5, in which the building period was calculated using Eq. (3). The following can be seen—

The over-conservatism of adopting FB philosophy for collapse-prevention design is evident by the large disparity between the motion intensity needed to reach collapse (damage state D5) compared to the peak strength (D2). For example, for two-way walls with  $L \geq 2000$  mm the ratio of D5/D2 varies between 4 to 12, and for parapets with  $H \geq 500$  mm between 3 to 10. It should be noted however that the predicted capacity at D2 can be sensitive to the initial stiffness of the wall, whose value in these analyses has been based on the assumption that the yield displacement is equal to 10% of the wall thickness.

Each of the code methods—even the exact peak floor acceleration technique (code method 3)—seems to unwittingly counteract the conservatism of FB philosophy, as seen from the fact that each one produces higher estimates of capacity compared to the D2 damage state. The reason is that the THA inherently incorporates dynamic amplification of the wall because of the finite stiffness in the elastic range (over  $\Delta \leq \Delta_{ry}$  in Figure 1), whereas the code methods ignore component amplification [ $a_c = 1$  in Eq. (1)] treating the wall as rigid. This compensating effect however still does not lead to reliable estimates of the actual capacity against collapse using the code approaches as seen by their general mismatch relative to the D5 damage state.

## Effect of building period

The reference analyses shown in parts (a) of Figures 4 and 5 were performed by estimating the building period with the simple code formula [Eq. (3)]. It is evident however that the building period has a major influence on the OOP wall fragility, as seen by comparing part (a) of these figures to part (b). In (b) the period was elongated by a factor of two, which is shown to have a generally detrimental effect on wall capacity as a result of dynamic interaction between the building and wall. Such period elongation could occur for example due to in-plane wall damage, or in buildings prone to torsional response as shown by analyses on typical Australian URM buildings performed by Bracchi (2017).

Consider the original building period in parts (a) of Figure 4 and 5. Comparing the code methods to the collapse damage state shows that even if we allow for a reasonable level of ‘design conservatism’ by adopting the 5% fractile values at the collapse prevention level (D5), the corresponding capacities are still considerably more favourable (economical) than by using the ‘exact’ FB code method (method 3). However, for an elongated building period [parts (b)], the dynamic interaction causes the FB predictions to become unsafe in certain regions, for both the parapet and two-way wall. This further highlights the unreliability of the code approaches.

### Other trends

**Effect of number of storeys and wall span ( $L$  or  $H$ ):** In general, a masonry component (wall or parapet) in a taller building is more vulnerable to OOP collapse than the same component in a shorter building (Figures 4 and 5). Similarly a wall with a longer span is typically more vulnerable than a shorter wall. These trends are unsurprising and stem respectively from the fact that a taller building will typically cause greater amplification at the component level, and a longer span leads to a lower force capacity. However the trends do not always hold—in certain instances the opposite is observed, which can be explained by the complex dynamic interaction between the ground motion and the building, and between the floor motion and the wall.

**Influence of two-way bending:** A wall in one-way vertical bending can be considered equivalent to a two-way wall with a sufficiently large length. Therefore the benefit that results from two-way bending is demonstrated in Figure 4 by looking at the enhancement of capacity from a reduction in the wall length; this improvement is observed for both force- and displacement-based assessment.

## CONCLUSION

Reliable out-of-plane wall assessment continues to be a major challenge for design engineers. This paper has demonstrated a technique for generating analytical fragility curves for OOP wall components using a nonlinear THA to obtain realistic estimates of expected behaviour based on current best practice.

The results indicate that:

- DB design offers considerable economy over conventional FB design; it can be used to demonstrate the adequacy of wall components in scenarios where FB design suggests them to be unsafe. This leads to a more reliable representation of seismic risk and therefore a less wasteful use of resources in deploying seismic strengthening.
- Walls that undergo two-way bending also exhibit considerably greater seismic resilience than vertically spanning walls and thus the additional benefit should not be ignored in design.
- The analyses also indicate however that fragility of OOP wall components is highly dependent on dynamic interaction with the building; an elongation of the building period that could arise due to in-plane wall damage can substantially reduce the intensity of

shaking that the component can withstand—under such conditions the FB methods prescribed by AS 1170.4 can lead to unsafe predictions. This is an area warranting further research.

## ACKNOWLEDGEMENTS

The authors gratefully acknowledge the financial support of the Australian Research Council (through grants DP160102070 and DP190100797) and the Bushfire and Natural Hazards CRC for the work presented in this paper. The conclusion and opinions expressed herein are those of the authors and not necessarily of the sponsors.

## REFERENCES

- Bracchi, S. (2017). “Improved tools and strategies for the derivation of analytical fragility curves of existing URM buildings”, PhD Thesis, University of Pavia.
- Burton, C., Vaculik, J., Visintin, P., M., G., and Sheikh, A. (2019). “Pull out capacity of chemical and mechanical anchors in clay masonry under quasi-static, cyclic and impact loading.” Proc., Australian Earthquake Engineering Society Conference.
- D'Ayala, D., and Speranza, E. (2003). “Definition of collapse mechanisms and seismic vulnerability of historic masonry buildings.” *Earthquake Spectra*, 19(3), 479-509.
- Derakhshan, H., Lucas, W. D., and Griffith, M. C. (2018). “In-situ seismic verification of non-structural components of unreinforced masonry buildings.” *Australian Journal of Structural Engineering*, 19(1), 44-58.
- Doherty, K., Griffith, M. C., Lam, N., and Wilson, J. (2002). “Displacement-based seismic analysis for out-of-plane bending of unreinforced masonry walls.” *Earthquake Engineering and Structural Dynamics*, 31(4), 833-850.
- Lagomarsino, S. (2015). “Seismic assessment of rocking masonry structures.” *Bulletin of Earthquake Engineering*, 13(1), 97-128.
- NZSEE (2017). “The Seismic Assessment of Existing Buildings – C8 Unreinforced Masonry Buildings”, New Zealand Society for Earthquake Engineering.
- Standards Australia (2018). AS1170.4–2007(R2018) Structural design actions Part 4: Earthquake actions in Australia, SA, Sydney, NSW.
- Vaculik, J., and Griffith, M. C. (2008). “Time-history analysis for unreinforced masonry walls in two-way bending.” Proc., 14th World Conference on Earthquake Engineering.
- Vaculik, J., and Griffith, M. C. (2017). “Out-of-plane load–displacement model for two-way spanning masonry walls.” *Engineering Structures*, 141, 328–343.